ChemComm

COMMUNICATION

View Article Online
View Journal | View Issue

Cite this: *Chem. Commun.*, 2015, 51, 2547

Received 6th November 2014,
Accepted 23rd December 2014

DOI: 10.1039/c4cc08888c

www.rsc.org/chemcomm

Decontamination of nanoparticles from aqueous samples using supramolecular gels†

Amit Patwa,[ab] Jérôme Labille,[c] Jean-Yves Bottero,[c] Alain Thiéry[d] and Philippe Barthélémy*[ab]

The growing use of nanomaterials and their associated risks necessitate the emergence of efficient decontamination systems. The main objective of this study is to develop a new prototype based on artificial supramolecular hydrogel capable of removing nanoparticle (NP) waste and nanomaterial by-products from aqueous suspensions. We demonstrate the high trapping efficacy of the low-molecular-weight gelators (LMWG) for very small particles (quantum dots (QDs), gold nanoparticles (AuNPs), TiO_2 nanoparticles (TiO_2-NPs), below 50 nm in diameter) from aqueous suspensions. The performance levels of removing nanoparticles from contaminated effluents could lead to a competitive alternative to filtration and dialysis devices.

Nanomaterials exhibit novel properties that offer a variety of new applications in different areas such as electronics,[1] biomedicine,[2–4] pharmaceuticals, cosmetics, energy,[5] environment,[6] catalysts and materials. Owing to the potential benefits of nanotechnologies in various fields, there is a significant increase in the production and utilization of nanomaterials. The rapidly growing application of nano-products results in a potentially increased exposure of humans and environment to nanomaterials. The high reactivity of these nanomaterials may lead to adverse effects on biological systems, including human[7] and ecological[8] spheres. Consequently, the arrival on the market of nano-products raises crucial issues dealing with human/environment risk assessment and potentially associated contaminations.[9] Keeping in mind the risk associated with nanomaterials, it is essential to develop efficient decontamination methods to remove or subtract nano-particles (NPs) from contaminated wastes and environments including aqueous samples and surfaces. Surprisingly, despite the strong demand only a few types of decontamination devices (*i.e.* coagulation and flocculation of NPs by organic polymers,[10] polyaluminium chloride[11]) have been developed so far.[12]

In this context, we hypothesized that the use of the low-molecular-weight gelators (LMWGs) could serve as temporary scaffolds allowing nanoparticles to be trapped. These LMWGs offer several advantages to synthetic polymeric gels as they possess properties that are non-achievable by polymers.[13–16] For example, water gelation by small molecules allows a rapid response of the gels to external stimuli, inherent gel–sol reversibility due to the non-covalent nature of the gel formation, and easy elimination after use thanks to the gel-to-sol transition. Our interest lies in using nucleoside-based amphiphiles capable of forming supramolecular systems. To this end, a large family of glycosylated-nucleoside-based amphiphiles featuring lipid (GNLs) have been synthesized and characterized.[17–22] We discovered that these molecules form nanostructured hydrogels and organogels.[17,18] In the present study, we have used a glycosylated-nucleoside fluorinated amphiphile (GNF), as a trapping scaffold to address the nano-waste issue.[18] We demonstrate the ability of nanostructured supramolecular hydrogels, offered by the GNF, to entrap nanoparticles from aqueous samples (Fig. 1).

In order to evaluate the decontamination properties of a GNF, the accumulation of various NPs in the GNF hydrogel have been investigated. Initially, NPs derived from water soluble lipid-encapsulated QDs (previously synthesized in our lab), were suspended in water to prepare the contaminated samples.[23] In a typical experiment, the GNF hydrogel was prepared and incubated in the presence of the QD suspension. After allowing this mixture to settle down for 48 h in the dark, a gel along with the supernatant liquid phase was observed (Fig. 2A). The supernatant liquid was separated from the gel (Fig. 2B). As hypothesized, visualization under UV radiation (λ_{max} = 312 nm) revealed that all the encapsulated QDs were

[a] *Univ. Bordeaux, ARNA laboratory, F-33000 Bordeaux, France*
[b] *INSERM, U869, ARNA laboratory, F-33000 Bordeaux, France. E-mail: philippe.barthelemy@inserm.fr; Fax: +33 5 57 57 10 15; Tel: +33 5 57 57 48 53*
[c] *CEREGE Europole de l'Arbois BP 80, Aix en Provence F-13545, France*
[d] *IMBE UMR CNRS 7263, Aix-Marseille Université, Aix en Provence F-13545, France*

† Electronic supplementary information (ESI) available: Materials and method, the general procedure for hydrogel formation to entrap nanoparticles, fluorescence spectroscopy, UV-visible spectroscopy, TEM experiment. See DOI: 10.1039/c4cc08888c

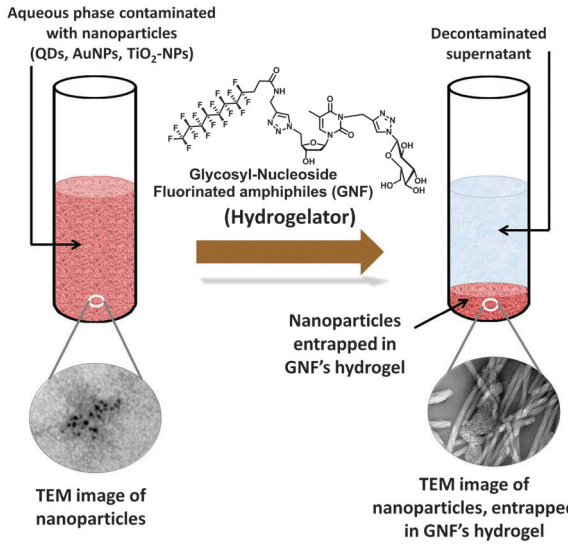

Fig. 1 Schematic illustration of the removal of the NPs from aqueous samples using GNF hydrogelators.

entirely entrapped in the GNF hydrogel (red fluorescence) while no QDs were left behind in the supernatant liquid (no red fluorescence) (Fig. 2C). The fluorescence spectra of the encapsulated-QD solution and supernatant liquid (after hydrogel formation) were recorded. No emission peak corresponding to QDs was observed, indicating the absence of NPs in the supernatant (Fig. 2D). Interestingly, transmission emission microscopy (TEM) images of the gel phase revealed that the QDs were trapped in the nanostructured hydrogel matrix (Fig. 2E) (for a better resolution see Fig. S4, ESI†).

To further investigate the trapping capability of the GNF hydrogel, similar sets of experiments with borohydride-reduced lysine-capped gold nanoparticles (AuNPs) were carried out.[24] As mentioned earlier, the GNF hydrogel was prepared and incubated in the presence of lysine-capped AuNP solution (Fig. 3A). After 48 h of incubation at room temperature, a pink colored gel appeared along with a colourless supernatant liquid, indicating that all the lysine-capped AuNPs were trapped in the hydrogel (Fig. 3B). To confirm the absence of lysine-capped AuNPs in the supernatant liquid, the gel phase was removed (Fig. 3C) and the UV-visible absorbance spectra of the

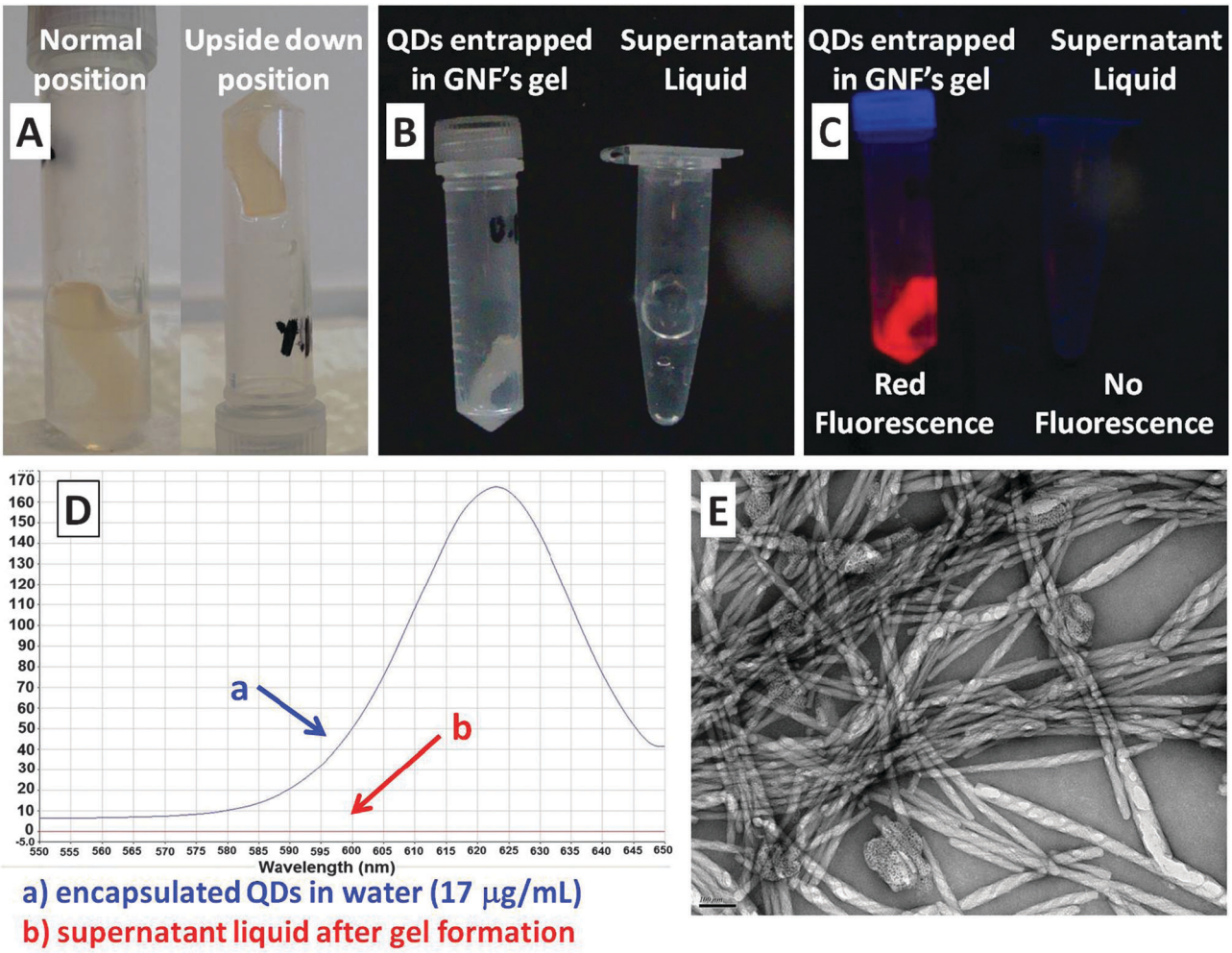

Fig. 2 QDs entrapped in GNF's hydrogel (0.1% (w/v)) (A) with supernatant liquid in normal and upside down position (B) under normal visualization (C) under UV visualization (λ_{max} = 312 nm) (D) fluorescence spectra (E) TEM image (scale: 100 nm).

supernatant were recorded. A strong absorption peak at 510 nm corresponding to the lysine-capped AuNPs (green curve, Fig. 3D) was observed and no such absorption peak was observed for the supernatant liquid (dark blue curve, Fig. 3D). This indicates that a complete removal of lysine-capped AuNPs by the GNF hydrogel from the aqueous suspension had been achieved. A TEM image of the gel phase shows that lysine-capped AuNPs were trapped as aggregates in the gel network (Fig. 3E) (for a better resolution see Fig. S5, ESI†). Similar experiments were carried out with borohydride-reduced AuNPs (not lysine-capped). UV-visible absorption profile for borohydride-reduced AuNPs (not lysine-capped) and supernatant liquid after hydrogel formation were recorded (red and sky blue curves respectively, Fig. 3D).

Next, to explore the versatility of the GNF hydrogel to trap the NPs in the aqueous suspension, the experiments were carried out with negatively charged titanium dioxide nanoparticles (TiO_2-NPs). TiO_2-NP solution of the required concentration (100 mg L^{-1} in 0.001 M NaCl) was prepared from commercially available solution (172.4 g L^{-1} in water). As usual, the GNF was dissolved in TiO_2-NP solution (Fig. 4A). To our surprise, TiO_2-NPs aggregated quickly after the dissolution of GNF (<5 min) and the solution changed its appearance from transparent to hazy (Fig. 4B). With time, more TiO_2-NPs started aggregating resulting in the increase in the particle size. After allowing the solution to stand for 2 h, all the TiO_2-NPs were trapped in the hydrogel and settled down leaving behind the transparent supernatant liquid (Fig. 4C). The UV-visible absorbance spectra of the supernatant liquid (red curve, Fig. 4D) were recorded to measure the concentration of TiO_2-NPs left

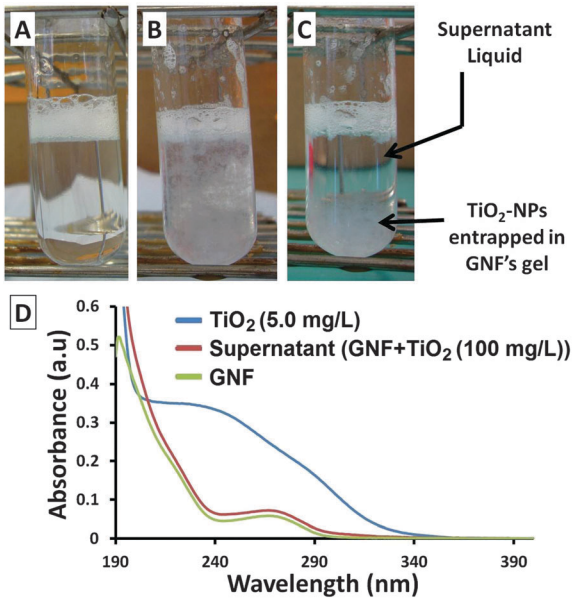

Fig. 4 TiO_2 with GNF's hydrogel (0.1% (w/v)) (A) immediately after mixing (B) aggregation after 5–10 min (C) aggregation and settling down after 2 h (D) UV-Vis absorption spectra.

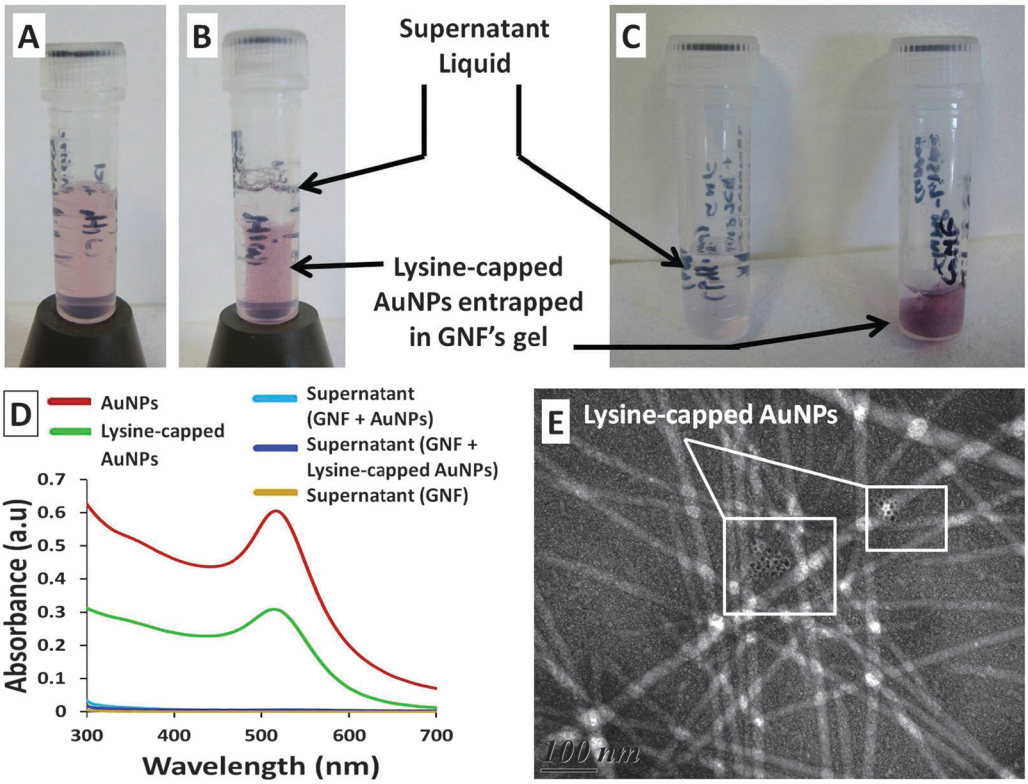

Fig. 3 Lysine-capped AuNPs with GNF (0.1% (w/w)) (A) immediately after mixing (B) hydrogel formation after 48 h (C) supernatant liquid and hydrogel separated (D) UV-Vis absorption spectra (E) TEM image (scale: 100 nm).

behind and compared it with the UV-visible profile of TiO_2-NPs solution (blue curve, Fig. 4D). No absorbance peak, corresponding to TiO_2-NPs, was observed in the case of the supernatant liquid (red curve, Fig. 4D) indicating that all the TiO_2-NPs were aggregated in the GNF hydrogel. TiO_2-NP samples (5.0 mg L^{-1}) were used to obtain the standard UV-visible absorbance profile (blue curve, Fig. 4D).

Finally, the concentration of the GNF left behind in the supernatant liquid (after hydrogel formation) was measured using UV-visible absorbance spectroscopy. These experiments revealed that only 0.8–1.1% of the total GNF was left behind in the supernatant liquid (*i.e.* for 2 mg mL^{-1} GNF-hydrogel, the concentration of GNF in the supernatant liquid was 0.02 mg mL^{-1}). Regarding the toxicity of the GNF left behind in the supernatant liquid, we have already reported the biocompatibility of the GNF-based hydrogels with cells and tissues which showed that a similar amount of the soluble GNF did not have any cytotoxic effects.[17,25]

One possible explanation for the unique trapping properties of the supramolecular gel would be a thermodynamically favorable evolution of the system. Indeed, the interactions of the nanoparticles with the 3D network of the gel would lead to a more stable state corresponding to nanoparticles attached to the supramolecular self-assemblies.

In summary, a facile and general method for the decontamination of aqueous samples containing nanoparticles has been reported. By using nanostructured gels based on a low molecular weight gelator, the GNF, the removal of nanoparticles from aqueous colloidal suspensions was successfully achieved at room temperature. To our surprise, the neutral GNF based hydrogel shows high trapping efficacy for very small particles, including positive (QDs, AuNPs), and negative TiO_2-NPs nanoparticles, below 50 nm in diameter. The investigation described in this study seeks to move beyond the past studies of decontamination systems involving membranes or flocculation systems. The novelty of this process is illustrated by the very limited literature concerning decontamination applications of NPs. To date, there is no filtration–flocculation system on the market that is capable of removing NPs quantitatively from waste. The performance levels observed for supramolecular gels in removing NPs from contaminated effluents could open many new industrial opportunities.

The authors acknowledge financial support from the French National Research Agency (ANR) in the framework of its program Emergence ''NanoDeconGels'' ANR-12-EMMA-0008.

Notes and references

1 D. Wei, M. Obstbaum, M. Ribow, C. H. Back and G. Woltersdorf, *Nat. Commun.*, 2014, **5**, 3768.
2 J. Yao, M. Yang and Y. Duan, *Chem. Rev.*, 2014, **114**, 6130–6178.
3 G. Saez, X. Moreau, L. De Jong, A. Thiéry, C. Dolain, I. Bestel, C. Di Giorgio, M. De Méo and P. Barthélémy, *Nano Today*, 2010, **5**, 251–253.
4 L. H. Reddy, J. L. Arias, J. Nicolas and P. Couvreur, *Chem. Rev.*, 2012, **112**, 5818–5878.
5 C. Cheng and H. J. Fan, *Nano Today*, 2012, **7**, 327–343.
6 N. C. Mueller and B. Nowack, *Elements*, 2010, **6**, 395–400.
7 A. Nel, T. Xia, L. Mädler and N. Li, *Science*, 2006, **311**, 622–627.
8 M. Farré, K. Gajda-Schrantz, L. Kantiani and D. Barceló, *Anal. Bioanal. Chem.*, 2009, **393**, 81–95.
9 M. R. Wiesner and J.-Y. Bottero, *C. R. Phys.*, 2011, **12**, 659–668.
10 M. Bizi, *Nat. Sci.*, 2012, **4**, 372–385.
11 M. R. Chang, D. J. Lee and J. Y. Lai, *J. Environ. Manage.*, 2007, **85**, 1009–1014.
12 P. Charles, M. Bizi, P. Guiraud, J. Labille and M.-L. Janex-Habibi, *Proceedings of Water Quality Technology Conference and Exposition*, Phoenix, Arizona, USA, 2011, pp. 995–1004.
13 K. J. C. Van Bommel, C. Van Der Pol, I. Muizebelt, A. Friggeri, A. Heeres, A. Meetsma, B. L. Feringa and J. Van Esch, *Angew. Chem., Int. Ed.*, 2004, **43**, 1663–1667.
14 S. Dong, Y. Luo, X. Yan, B. Zheng, X. Ding, Y. Yu, Z. Ma, Q. Zhao and F. Huang, *Angew. Chem., Int. Ed.*, 2011, **50**, 1905–1909.
15 X. Yan, D. Xu, X. Chi, J. Chen, S. Dong, X. Ding, Y. Yu and F. Huang, *Adv. Mater.*, 2012, **24**, 362–369.
16 S. Dong, B. Zheng, D. Xu, X. Yan, M. Zhang and F. Huang, *Adv. Mater.*, 2012, **24**, 3191–3195.
17 G. Godeau and P. Barthélémy, *Langmuir*, 2009, **25**, 8447–8450.
18 G. Godeau, C. Brun, H. Arnion, C. Staedel and P. Barthélémy, *Tetrahedron Lett.*, 2010, **51**, 1012–1015.
19 L. Latxague, S. Ziane, O. Chassande, A. Patwa, M.-J. Dalila and P. Barthélémy, *Chem. Commun.*, 2011, **47**, 12598–12600.
20 L. Latxague, M.-J. Dalila, A. Patwa, S. Ziane, O. Chassande, G. Godeau and P. Barthélémy, *C. R. Chim.*, 2012, **15**, 29–36.
21 C. Dolain, A. Patwa, G. Godeau and P. Barthélémy, *Appl. Sci.*, 2012, **2**, 245–259.
22 L. Latxague, A. Patwa, E. Amigues and P. Barthélémy, *Molecules*, 2013, **18**, 12241–12263.
23 A. Aimé, N. Beztsinna, A. Patwa, A. Pokolenko, I. Bestel and P. Barthélémy, *Bioconjugate Chem.*, 2013, **24**, 1345–1355.
24 P. R. Selvakannan, S. Mandal, S. Phadtare, R. Pasricha and M. Sastry, *Langmuir*, 2003, **19**, 3545–3549.
25 S. Ziane, S. Schlaubitz, S. Miraux, A. Patwa, C. Lalande, I. Bilem, S. Lepreux, B. Rousseau, J.-F. Le Meins, L. Latxague, P. Barthélémy and O. Chassande, *Eur. Cells Mater.*, 2012, **23**, 147–160.

